

# COUPLING AND POLARIZATION CONTROL IN A MM-WAVE UNDULATOR\*

F. Toufexis<sup>†1</sup>, J. Neilson, S.G. Tantawi, SLAC, Menlo Park, CA 94025

<sup>1</sup>Also at Department of Electrical Engineering, Stanford University, Stanford, CA 94305.

## Abstract

To reduce the linac energy required for an FEL radiating at a given wavelength, and hence its size, a smaller undulator period with sufficient field strength is needed. Previous work from our group successfully demonstrated a microwave undulator at 11.424 GHz using a corrugated cylindrical waveguide operating in the HE<sub>11</sub> mode. Scaling down the undulator period using this technology poses the challenge of confining and coupling the electromagnetic fields while maintaining overmoded features for power handling capability and electron beam wakefield mitigation. We have designed a mm-wave undulator cavity at 91.392 GHz. This undulator requires approximately 1.4 MW for sub-microsecond pulses to generate an equivalent K value of 0.1. Transferring such amounts of power in mm-wave frequencies requires overmoded corrugated waveguides, and coupling through irises creates excessive pulsed heating. We have designed a novel mode launcher that allows coupling power from a highly overmoded corrugated waveguide to the undulator through the beam pipe. Additionally, this mode launcher can be used along with grating polarizers to control the polarization of the produced light.

## INTRODUCTION

Synchrotron light sources and Free-Electron Lasers (FELs) are very large and expensive facilities. These facilities typically employ permanent magnet undulators, which present several limitations on how short their period can be while maintaining reasonable field strength and beam aperture. In order to reduce the undulator period, and hence the size and cost of light source facilities, several alternatives to traditional permanent magnet undulators have been investigated, one of which is microwave undulators [1]. Microwave undulators present the advantage of fast control of the polarization of the produced light. A microwave undulator has been successfully demonstrated at 11.424 GHz [1].

Polarization control in synchrotron light sources and FELs has several applications in the study of magnetic materials [2–4] and biological molecules [5,6], including drugs [7]. Circularly polarized light has been generated in synchrotron light sources using off-plane bending magnet radiation [8] and a variety of insertion devices [9]. Circularly polarized ultraviolet and soft X-ray light has also been generated in FELs [10, 11]. Recently a delta undulator [12] was installed in the Linac Coherent Light Source (LCLS) at SLAC to pro-

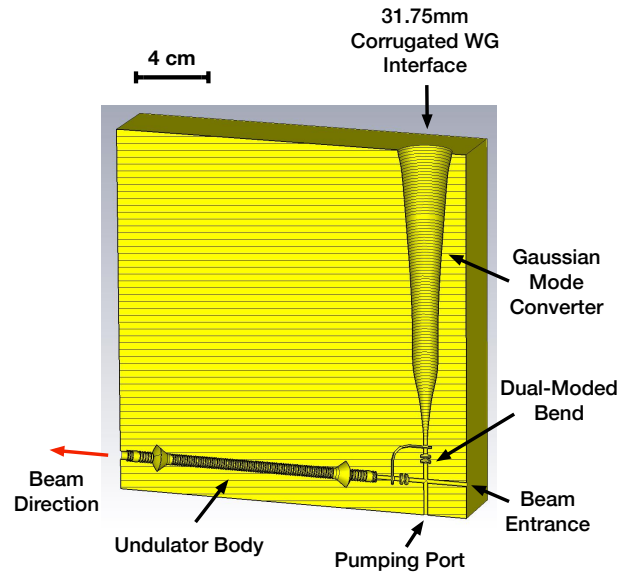


Figure 1: Millimeter-wave undulator with coupling system cross-section.

duce even higher energy polarized X-rays [13]. The time required for the LCLS delta undulator to switch polarization between left and right was 35 s [13]. Other methods of producing polarized soft X-rays include high harmonic generation sources [14], which are not efficient in the X-ray regime, and using magnetized films [15, 16], which are limited to specific wavelengths, low intensity, and only up to 60% circular polarization.

We have designed a novel mm-wave undulator cavity at 91.392 GHz [17]. In this work we report the design of the coupling system for the undulator, which preserves the polarization of the input and has large apertures for pumping and for the electron beam to enter the undulator. Figure 1 shows the undulator with the coupling system. Power is transferred to the undulator from a mm-wave source through an overmoded corrugated waveguide in order to minimize the losses. The standard rectangular waveguide WR10 has more than 3 dB m<sup>-1</sup> attenuation [18], while a 31.75 mm corrugated waveguide has approximately 0.004 dB m<sup>-1</sup> attenuation [19]. Additionally, for the device to operate under vacuum, a vacuum break with a flange is required. Due to the small dimensions of WR10, it is very difficult to implement a reliable vacuum flange for this waveguide. We therefore decided to place the vacuum break at the interface with the corrugated waveguide, where a standard flange exists. The coupling system consists of a Gaussian to cylindrical TE<sub>11</sub> mode converter and a dual-moded bend. These components

\* This project was funded by U.S. Department of Energy under Contract No. DE-AC02-76SF00515, and the National Science Foundation under Contract No. PHY-1415437.

<sup>†</sup> ftouf@stanford.edu

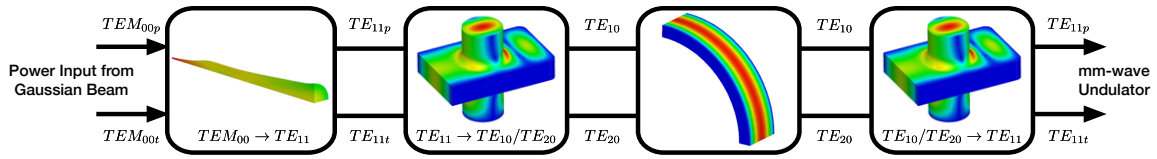


Figure 2: Coupling system schematic.

and the respective mode conversions are shown schematically in Fig. 2.

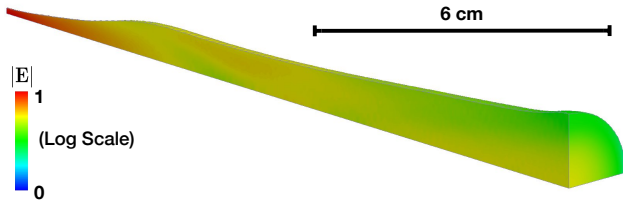


Figure 3: Surface electric field profile of the Gaussian to  $TE_{11}$  mode converter (log scale).

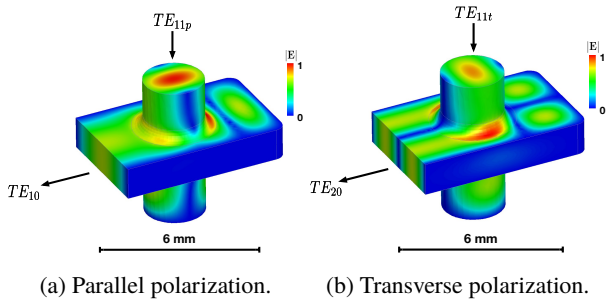


Figure 4: Surface electric field for the cylindrical  $TE_{11}$  to rectangular  $TE_{10}/TE_{20}$ .

### COUPLING SCHEME DESIGN

#### Gaussian to $TE_{11}$ Mode Converter Design

The Gaussian to  $TE_{11}$  mode converter is used to convert a Gaussian  $TEM_{00}$  mode to a smooth-walled cylindrical waveguide  $TE_{11}$ . The smooth cylindrical waveguide is sized to only support  $TE_{11}$ . This mode converter is axisymmetric, and therefore the two polarizations  $TEM_{00p}$  and  $TEM_{00t}$  of the Gaussian mode convert to the equivalent polarizations in the cylindrical waveguide  $TE_{11p}$  and  $TE_{11t}$ . Figure 3 shows the Gaussian to  $TE_{11}$  mode converter. The complex Gaussian coupling factor is 0.99, the cross-polarization level is  $-23$  dB, the Gaussian beam waist is 0.94 cm, and the reflection coefficient from the cylindrical waveguide is 0.0028. This mode converter was synthesized using a Mode Matching Code [20] and the method described in [21]. At the Gaussian side of this mode converter there will potentially be a vacuum window, to isolate the vacuum system of the undulator from that of the RF transport lines.

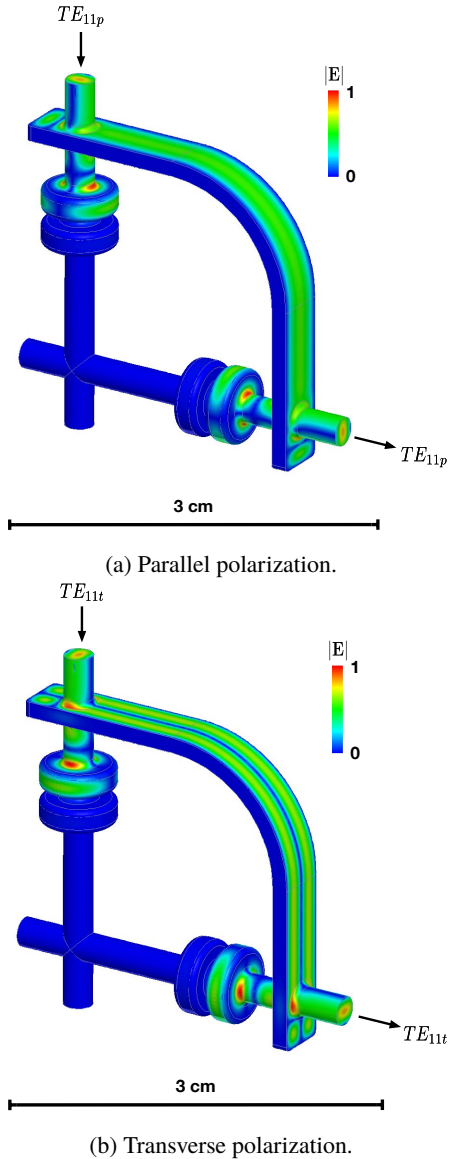


Figure 5: Surface electric field of the dual-moded bend.

#### Dual-Moded Bend Design

The  $TE_{11}$  coming from the Gaussian to  $TE_{11}$  mode converter is subsequently converted to a rectangular waveguide mode. The rectangular waveguide is sized to only support  $TE_{10}$  and  $TE_{20}$ . As shown in Fig. 4, the cylindrical  $TE_{11p}$  is converted to the rectangular  $TE_{10}$  and the cylindrical  $TE_{11t}$  is converted to the rectangular  $TE_{20}$ . The bottom of this mode converter is opened by adding chokes. We designed a two-piece choke, shown in Fig. 5 to account for manufactur-

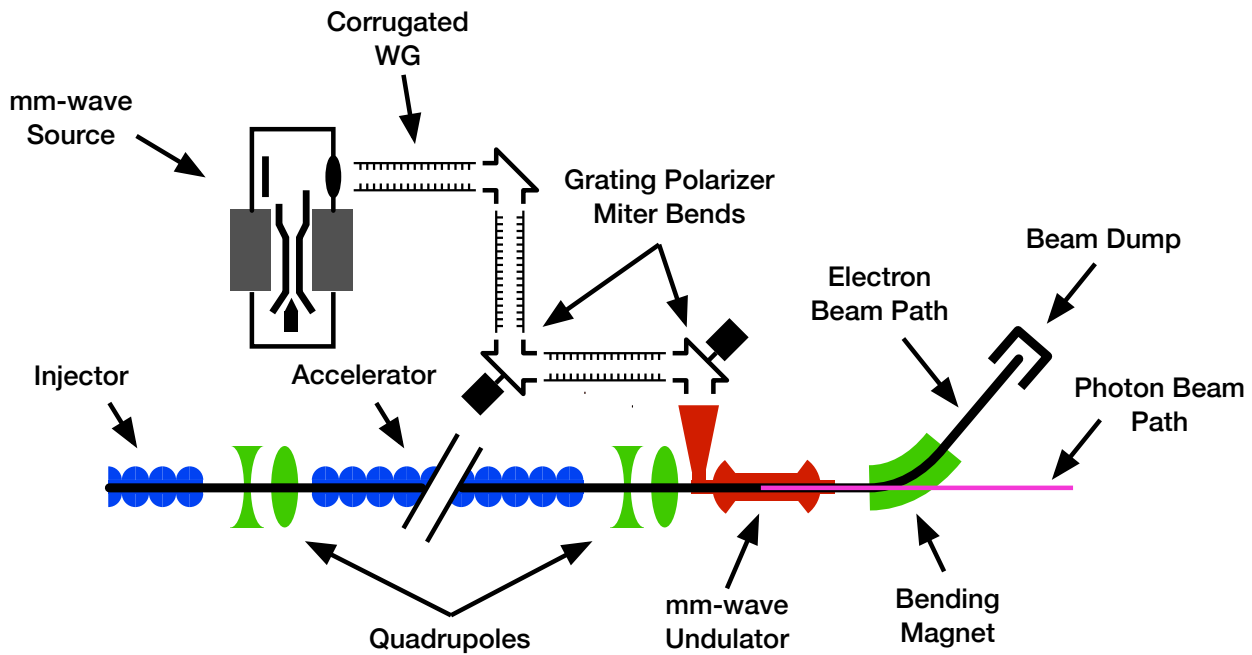


Figure 6: Light source schematic utilizing the mm-wave undulator with polarization control.

ing tolerances. The two rectangular waveguide modes are then transmitted through an E-plane bend, connected to a second rectangular-to-cylindrical mode converter.

Figure 5 shows the system of the two rectangular to cylindrical mode converters, the rectangular bend, and the chokes. The system is optimized so that there is no phase slippage between the two polarizations of  $TE_{11}$  at the end of the mode converter. As can be seen in Fig. 5, each polarization of  $TE_{11}$  at the input cylindrical waveguide is transmitted unaltered to the output cylindrical waveguide. The use of chokes allows for two orthogonally placed through holes, one for the electron beam to enter the undulator, and one to pump the vacuum space of the mode converter. For a 10 MW power flow through this mode converter, the peak magnetic field on the metal surface is  $282 \text{ kA m}^{-1}$ . From [22] the peak pulsed surface heating for 250 ns RF pulses is  $48^\circ\text{C}$ , which is considered safe for copper [23]. Figure 1 shows the entire system assembly with the undulator.

### POLARIZATION CONTROL

Polarization of the produced light is directly controlled by the polarization of the Gaussian mode incident to the undulator system of Fig. 1.  $TE_{11}$  gyro traveling wave tubes such as the one reported in [24–26] could be modified to produce variable polarization by having two input signals separately coupled to the two polarization of the  $TE_{11}$ . A change of polarization between left and right could be achieved between RF pulses, the spacing of which is typically on the order of milliseconds. Another method to control and change the polarization is the use of a pair of grating polarizer miter bends with motors [27]. In this case, the speed of polarization change is limited by the motors and is on the order of

a second. Figure 6 shows the schematic of a light source utilizing the mm-wave undulator with polarization control.

### CONCLUSION

We reported the design of a novel coupling scheme for a mm-wave undulator at 91.392 GHz. Power is transferred from the mm-wave source through a 31.75 mm corrugated waveguide. The  $HE_{11}$  in the corrugated waveguide is converted into cylindrical  $TE_{11}$ , and then bent  $90^\circ$  while preserving polarization. Power is coupled into the undulator through the beam pipe. This coupling scheme allows for fast change of polarization between left and right on the order of a second using grating polarizers, and on the order of milliseconds through the mm-wave source. In comparison, the time to switch polarization between left and right for the LCLS delta undulator is 35 s.

### REFERENCES

- [1] S. Tantawi *et al.*, “Experimental Demonstration of a Tunable Microwave Undulator,” *Phys. Rev. Lett.*, vol. 112, no. 16, p. 164802, Apr. 2014.
- [2] G. Schutz *et al.*, “Absorption of circularly polarized x rays in iron,” *Phys. Rev. Lett.*, vol. 58, no. 7, pp. 737–740, Feb. 1987.
- [3] C. E. Graves *et al.*, “Nanoscale spin reversal by non-local angular momentum transfer following ultrafast laser excitation in ferrimagnetic GdFeCo,” *Nature Materials*, vol. 12, no. 4, pp. 293–298, Mar. 2013.
- [4] D. J. Higley *et al.*, “Femtosecond X-ray magnetic circular dichroism absorption spectroscopy at an X-ray free electron laser,” *Review of Scientific Instruments*, vol. 87, no. 3, p. 033110, 2016.

- [5] N. Bowering *et al.*, “Asymmetry in Photoelectron Emission from Chiral Molecules Induced by Circularly Polarized Light,” *Phys. Rev. Lett.*, vol. 86, no. 7, pp. 1187–1190, Feb. 2001.
- [6] U. Hergenbahn *et al.*, “Photoelectron circular dichroism in core level ionization of randomly oriented pure enantiomers of the chiral molecule camphor,” *The Journal of Chemical Physics*, vol. 120, no. 10, pp. 4553–4556, 2004.
- [7] L. A. Nguyen *et al.*, “Chiral Drugs: An Overview,” *International Journal of Biomedical Science : IJBS*, vol. 2, no. 2, pp. 85–100, Jun. 2006.
- [8] C. T. Chen *et al.*, “Soft-x-ray magnetic circular dichroism at the  $L_{2,3}$  edges of nickel,” *Phys. Rev. B*, vol. 42, no. 11, pp. 7262–7265, Oct. 1990.
- [9] P. Elleaume, “Generation of various polarization states from insertion devices: A review,” *Review of Scientific Instruments*, vol. 60, no. 7, pp. 1830–1833, 1989.
- [10] O. A. Shevchenko *et al.*, “The VUV/UV OK-5 Duke storage ring FEL with variable polarization,” in *PACS2001. Proceedings of the 2001 Particle Accelerator Conference (Cat. No.01CH37268)*, 2001, pp. 2833–2835 vol.4.
- [11] A. E *et al.*, “Two-stage seeded soft-X-ray free-electron laser,” *Nature Photonics*, vol. 7, no. 11, pp. 913–918.
- [12] A. B. Temnykh, “Delta undulator for Cornell energy recovery linac,” *Phys. Rev. ST Accel. Beams*, vol. 11, no. 12, p. 120702, Dec. 2008.
- [13] A. A. Lutman *et al.*, “Polarization control in an X-ray free-electron laser,” *Nature Photonics*, vol. 10, no. 7, pp. 468–472, May 2016.
- [14] B. Vodungbo *et al.*, “Polarization control of high order harmonics in the EUV photon energy range,” *Opt. Express*, vol. 19, no. 5, pp. 4346–4356, Feb. 2011.
- [15] B. Pfau *et al.*, “Magnetic imaging at linearly polarized x-ray sources,” *Opt. Express*, vol. 18, no. 13, pp. 13 608–13 615, Jun. 2010.
- [16] T. Wang *et al.*, “Femtosecond Single-Shot Imaging of Nanoscale Ferromagnetic Order in Co/Pd Multilayers Using Resonant X-Ray Holography,” *Phys. Rev. Lett.*, vol. 108, no. 26, p. 267403, Jun. 2012.
- [17] F. Toufexis and S. G. Tantawi, “A 1.75 mm Period RF-Driven Undulator,” in *Proc. of International Particle Accelerator Conference (IPAC’17), Copenhagen, Denmark, May 14-19, 2017*. Geneva, Switzerland: JACoW, May 2017.
- [18] I. Stil *et al.*, “Loss of WR10 waveguide across 70–116 GHz,” in *Proc. 22nd Int. Symp. Space Terahertz Technol*, 2012, pp. 1–3.
- [19] R. A. Olstad *et al.*, “Considerations in Selection of ECH System Transmission Line Waveguide Diameter for ITER,” *Journal of Physics: Conference Series*, vol. 25, no. 1, pp. 166–172, 2005.
- [20] J. M. Neilson *et al.*, “Determination of the resonant frequencies in a complex cavity using the scattering matrix formulation,” *IEEE Transactions on Microwave Theory and Techniques*, vol. 37, no. 8, pp. 1165–1170, Aug. 1989.
- [21] J. M. Neilson, “An improved multimode horn for Gaussian mode generation at millimeter and submillimeter wavelengths,” *IEEE Transactions on Antennas and Propagation*, vol. 50, no. 8, pp. 1077–1081, Aug. 2002.
- [22] V. A. Dolgashev, “High magnetic fields in couplers of X-band accelerating structures,” in *Proceedings of the 2003 Particle Accelerator Conference*, May 2003, pp. 1267–1269 Vol.2.
- [23] L. Laurent *et al.*, “Experimental study of rf pulsed heating,” *Phys. Rev. ST Accel. Beams*, vol. 14, no. 4, p. 041001, Apr. 2011.
- [24] R. S. Symons *et al.*, “An Experimental Gyro-TWT,” *IEEE Transactions on Microwave Theory and Techniques*, vol. 29, no. 3, pp. 181–184, Mar. 1981.
- [25] L. R. Barnett *et al.*, “Absolute instability competition and suppression in a millimeter-wave gyrotron traveling-wave tube,” *Phys. Rev. Lett.*, vol. 63, no. 10, pp. 1062–1065, Sep. 1989.
- [26] J. Wang *et al.*, “Simulation and Experiment of a Ku-Band Gyro-TWT,” *IEEE Transactions on Electron Devices*, vol. 61, no. 6, pp. 1818–1823, Jun. 2014.
- [27] J. L. Doane, “Grating polarizers in waveguide miter bends,” *International Journal of Infrared and Millimeter Waves*, vol. 13, no. 11, pp. 1727–1743, 1992.